Superconductivity of highly spin-polarized electrons in FeSe probed by ^{77}Se NMR

Molatta, S.; Opherden, D.; Wosnitza, J.; Opherden, L.; Zhang, Z. T.; Wolf, T.;
von Löhneysen, H.; Sarkar, R.; Biswas, P. K.; Grafe, H.-J.; Kühne, H.;

Originally published:

July 2021

Physical Review B 104(2021), 014504

DOI: https://doi.org/10.1103/PhysRevB.104.014504

Superconductivity of highly spin-polarized electrons in FeSe probed by ^{77}Se NMR

S. Molatta,[1,2] D. Opherden,[1,2] J. Wosnitza,[1,2] L. Opherden,[1,2] Z. T. Zhang,[1,3] T. Wolf,[4] H. v. Löhneysen,[4,5] R. Sarkar,[2] P. K. Biswas,[6] H.-J. Grafe,[7] and H. Kühne[1,*]

[1] *Hochfeld-Magnetlabor Dresden (HLD-EMFL) and Würzburg-Dresden Cluster of Excellence ct.qmat, Helmholtz-Zentrum Dresden-Rossendorf, 01328 Dresden, Germany*
[2] *Institut für Festkörper- und Materialphysik, TU Dresden, 01062 Dresden Germany*
[3] *Anhui Province Key Laboratory of Condensed Matter Physics at Extreme Conditions, High Magnetic Field Laboratory, Chinese Academy of Sciences, Hefei 230031, China*
[4] *Institut für Quantenmaterialien und -technologien, Karlsruher Institut für Technologie, 76021 Karlsruhe, Germany*
[5] *Physikalisches Institut, Karlsruher Institut für Technologie, 76049 Karlsruhe, Germany*
[6] *ISIS Facility, Rutherford Appleton Laboratory, Chilton, Didcot Oxon, OX11 0QX, United Kingdom*
[7] *IFW Dresden, Institute for Solid State Research, 01171 Dresden, Germany*

(Dated: June 25, 2021)

A number of recent experiments indicate that the iron-chalcogenide FeSe provides the long-sought possibility to study bulk superconductivity in the cross-over regime between the weakly coupled Bardeen–Cooper–Schrieffer (BCS) pairing and the strongly coupled Bose–Einstein condensation (BEC). We report on ^{77}Se nuclear magnetic resonance experiments of FeSe, focused on the superconducting phase for strong magnetic fields applied along the c axis, where a distinct state with large spin polarization was reported. We determine this high-field state as bulk superconducting with high spatial homogeneity of the low-energy spin fluctuations. Further, we find that the static spin susceptibility becomes unusually small at temperatures approaching the superconducting state, despite the presence of pronounced spin fluctuations. Taken together, our results clearly indicate that FeSe indeed features an unusual field-induced superconducting state of a highly spin-polarized Fermi liquid in the BCS-BEC crossover regime.

I. INTRODUCTION

The discovery of superconductivity in iron-based materials in 2008 opened a new avenue for the exploration of unusual superconducting states and phenomena in multiband superconductors, with wide possibilities for tuning the electronic ground states by variation of the material composition and the ensuing thermodynamic parameters [1–4]. At present, the binary iron-chalcogenide FeSe attracts a lot of research interest [5–15]. As to the Fermi-surface topology and energy scales in this material, there is one shallow hole pocket at the Γ point, and at least one electron pocket at the M point, both with remarkably small Fermi energies ($\varepsilon_F^e \approx 3$ meV and $\varepsilon_F^h \approx 10$ meV, respectively) [6, 16]. The superconducting gap energies are $\Delta_1 = 2.5$ meV and $\Delta_2 = 3.5$ meV, resulting in an unusually high ratio $\Delta/\varepsilon_F \approx 1$ and ≈ 0.3 for the electron and hole bands, respectively [6].

Despite its structural simplicity, FeSe yields a wealth of interesting phenomena. For example, a nematic transition, presumably induced by orbital ordering, occurs at about 90 K, where the C_4 rotational symmetry is broken, while the translational symmetry is preserved [8–11, 17]. A drastic increase of T_c can be achieved via hydrostatic pressure, or when growing thin films on specific substrates [18–20].

Further, very recently compelling evidence for the appearance of a Fulde-Ferrell-Larkin-Ovchinnikov (FFLO) state was found when the applied magnetic field is aligned parallel to the *ab* plane [15]. On the other hand, for fields perpendicular to the planes, the observation of an unusual superconducting phase with extremely high spin polarization, dubbed B phase, was reported based on measurements of thermal transport properties [21, 22]. Close to the upper critical field of superconductivity, all three relevant energy scales, i.e., those of the Fermi energy, the superconducting gap, and the Zeeman interaction, are of comparable magnitude, the combined action of which may lead to a significant modification of the underlying electronic system. For that reason, the condensation of electron pairs in the B phase is proposed to take place in the BCS (Bardeen–Cooper–Schrieffer) – BEC (Bose–Einstein-condensate) crossover regime, which bridges the two fundamental theories for the condensation of attractively coupled fermions. In this crossover regime, the average interparticle distance approaches the size of the interacting pairs, i.e., $k_F\xi \approx 1$, where k_F is the Fermi wave vector and ξ is the superconducting coherence length [21]. The resulting ground state is a strongly interacting superfluid, out of which new states of matter may emerge. The manifestation of preformed pairs with an associated pseudogap, existing at temperatures much higher than the actual condensation temperature, is a hallmark of the BCS-BEC crossover [23]. As the intrinsic energy scales in materials usually place the electronic interactions strictly in either the BCS or the BEC limit, little is known about bulk superconductivity in the crossover regime.

In this paper, we present ^{77}Se nuclear magnetic res-

* Corresponding author. E-mail: h.kuehne@hzdr.de

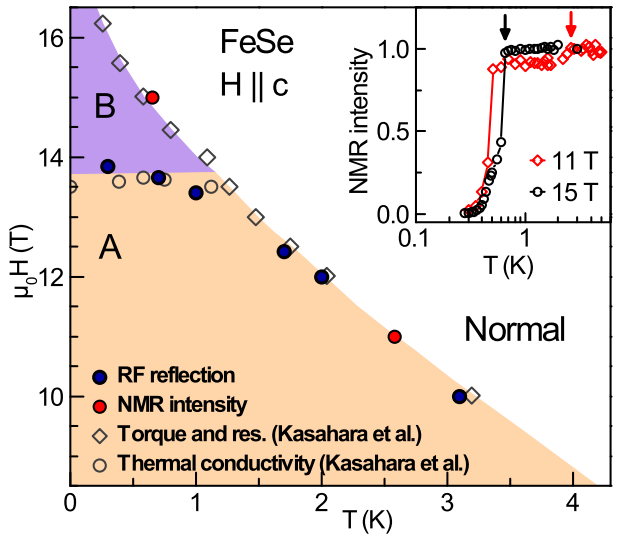

FIG. 1. Phase diagram of FeSe for fields parallel to the c axis. RF reflection experiments (blue circles) probe superconducting transitions to the A phase, in excellent agreement with magnetic torque, resistivity, and thermal-conductivity results [21], but are not sensitive to the onset of the B phase. Probing the ^{77}Se NMR intensity (red circles), however, reveals the transition to the B phase—like the A phase—as a bulk superconducting state. Inset: Temperature dependence of the ^{77}Se NMR signal intensity at 11 (red diamonds) and 15 T (black circles), evaluated as the integrated real part of the phase-corrected NMR frequency-domain spectrum, multiplied with temperature. The downward arrows indicate T_c at given field.

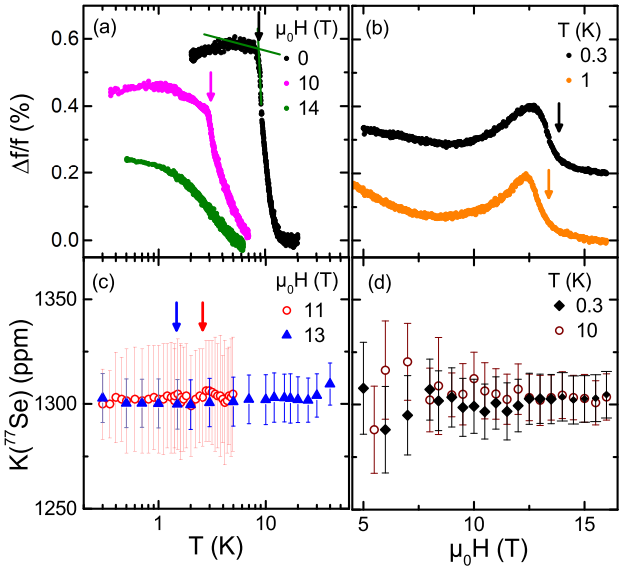

FIG. 2. (a) Temperature-dependent detuning of the NMR tank circuit. The arrows denote T_c, determined from linear fits, as exemplified for the 0 T curve. (b) Field-dependent detuning, with the data at 0.3 K shifted vertically for clarity. The arrows denote fields where an order-disorder transition of the vortex lattice, manifested as peaked enhancement, is completed. (c) Temperature dependence of the ^{77}Se Knight shift. The error bars are given by the spectral linewidth, the arrows denote T_c. (d) Field dependence of the ^{77}Se Knight shift at 0.3 and 10 K. The magnetic field was always applied parallel to the c axis.

onance (NMR) data of a high-quality single crystal of FeSe. The parameter range of our study covers magnetic fields between 5 and 16 T applied along the crystallographic c axis, and temperatures between 0.3 and 40 K. Our work mainly focuses on the electronic properties at low temperatures and close to the upper critical field of superconductivity, where the existence of the B phase was reported, thus constituting the first investigation of the local dynamic properties across the A-B transition in FeSe at the BCS-BEC crossover regime.

II. EXPERIMENTAL METHODS

The NMR coil with a vapor-grown FeSe single crystal [24], with dimensions of approximately 5.0 × 2.0 × 0.04 mm^3, was mounted on a single-axis rotator and placed directly in liquid ^{3}He inside a top-loading cryostat in a 16 T high-resolution magnet. The ^{77}Se NMR spectra were recorded using a commercial solid-state spectrometer with a 500 W power amplifier and a standard Hahn spin-echo pulse sequence. The ^{77}Se Knight shift, linewidth, and T_1 relaxation time were either measured in a top-tuned resonator configuration, using a typical $\pi/2$ pulse duration $t_{\pi/2} = 16$ μs and a power attenuation $\theta_{\pi/2} = 20$ dB, or in a bottom-tuned configuration, using $t_{\pi/2} = 29$ μs and $\theta_{\pi/2} = 36$ dB, with both configurations giving consistent results. The temperature-dependent intensity of the ^{77}Se NMR spectra, as shown in the inset of Fig. 1, was measured in the bottom-tuned resonator configuration, using a $\pi/2$ pulse duration $t_{\pi/2}$ = 5 μs and a power attenuation of 20 dB. Further details on the nutation response of the ^{77}Se nuclear magnetization are provided in the supplemental material [25]. The orientation of the magnetic field parallel to the crystallographic c axis was adjusted with an accuracy of about ±2° by probing the anisotropic frequency shift of the ^{77}Se spectra. To determine the superconducting phase diagram of our sample, we monitored changes of the complex radio-frequency (RF) reflection coefficient S11 at the NMR tank circuit, using a vector network analyzer. Here, the detuning of the resonance frequency indicates a relative change of sample volume penetration by the probing RF field.

The nuclear spin-lattice relaxation rate is defined as $1/T_1T \propto \sum_{q,n,m} F_{nm}(q)\chi''_{nm}(q, f_{res})/f_{res}$, with $n, m = x, y, z$. Here, F_{nm} denotes the hyperfine form factors and χ''_{nm} is the imaginary part of the dynamic electronic susceptibility. T_1 was measured via the saturation-recovery method and determined by fitting $M_z(\tau) = M_0\{1-\exp[-(\frac{\tau}{T_1})^\beta]\}$ to the recovery of the nuclear magnetization after saturation, where β is a stretching exponent that accounts for a distribution of relaxation times.

III. RESULTS AND DISCUSSION

The obtained results from the RF reflection measurements, shown in Fig. 1 as blue circles, are in very good agreement with previously reported data for the boundary of the A phase [21]. The characteristic temperatures and magnetic fields that determine the boundary of the A phase were extracted as intersection points of linear fits to the data above and below the respective slope changes in the temperature- and field-dependent sweeps, see Fig. 2(a). As shown in Fig. 2(a), in the temperature-dependent sweeps at fields corresponding to the A phase, the transition from the normal to the superconducting state is manifested as a pronounced change of slope, and we find $T_c = 8.7$ K at 0 T. At 14 T, however, upon crossing the transition to the B phase, no pronounced feature is observed.

In the field-dependent sweeps at low temperatures [see Fig. 2(b)], the resonance frequency at first monotonically decreases due to vortex formation in the Shubnikov phase, and shows a maximum at about 12.6 T and 0.3 K and at about 12.4 T and 1.0 K, closely below the transition between the A and B phase. The appearance of this maximum is attributed to an order-disorder transition of the vortex lattice, as was observed also by magnetic-torque measurements of FeSe, see supplemental information of [21]. Further, weak features in the data in Figs. 2(a) and 2(b), such as the kink at 10 T and 1 K in Fig. 2(a), are attributed to a principal lack of background compensation in the S11 RF reflection measurements.

Similar to the S11 RF reflection experiments, a change of the RF volume penetration at the transition to the superconducting state can be probed via the intensity of the NMR spectra, see inset of Fig. 1. At 11 T, the NMR intensity decreases by about 10% below $T_c = 2.6$ K due to vortex formation, and drops abruptly at around 0.5 K. The latter feature is attributed to a highly non-monotonic temperature dependence of the surface resistance below T_c, as revealed by RF impedance measurements [26]. In contrast, at 15 T, the intensity decreases sharply at $T_c \simeq 0.7$ K and reaches less than 1% of the normal-state value at lowest temperature. The nuclear spin-spin relaxation time T_2 is of the order 1 ms both in the normal and superconducting state. Therefore, an influence of T_2 effects on the temperature-dependent NMR intensity can be excluded. We note that the RF field amplitude is approximately several mT in the NMR intensity and a few ten μT in the RF reflection experiments, respectively. Apparently, the electronic properties of the B phase yield no pronounced electrodynamic response when probed via a weak RF field, but generate pronounced shielding effects when stimulated with a strong RF field. This statement is further supported by our ^{77}Se NMR nutation experiments in the normal and superconducting state [25], which provide more details on the RF volume penetration in the superconducting state at both 11 and 15 T. The origin of this behavior is unclear, so far.

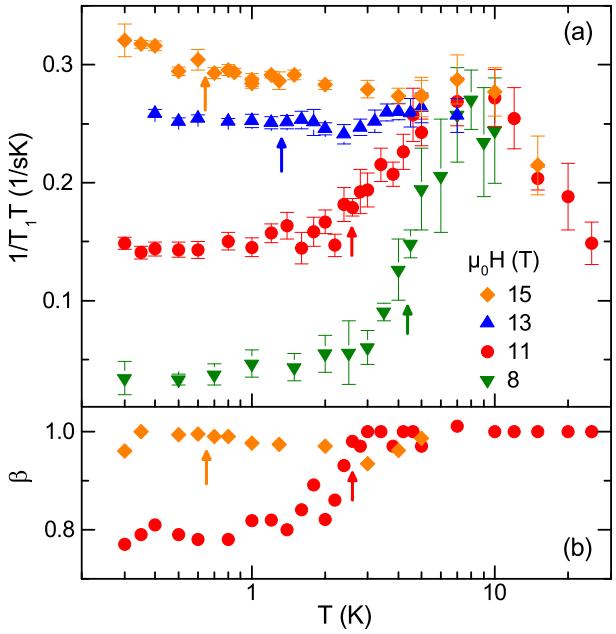

FIG. 3. (a) Temperature-dependent $1/T_1T$ of FeSe for fields parallel to the c axis. The arrows denote T_c as determined from the RF reflection and NMR intensity experiments, respectively. (b) Stretching exponent β of the T_1 relaxation as a function of temperature.

Having established the phase diagram, we next turn to our investigation of the intrinsic electronic properties, probed via NMR observables. In general, the NMR Knight shift is defined as $K = K_{\rm orb} + K_{\rm s}$, being composed of a constant orbital part $K_{\rm orb}$ and a spin part $K_{\rm s}$, defined as $K_{\rm s} = A_{hf} \cdot \chi$, with the hyperfine coupling A_{hf} and the electronic dc susceptibility χ. From previous ^{77}Se NMR results of FeSe above the nematic transition temperature, a hyperfine coupling of $A_{hf} = 3.77$ T/μ_B was reported [9]. This value is large compared to the hyperfine couplings of other nuclear isotopes used in the study of iron-based superconductors [27–30]. Hence, the ^{77}Se Knight shift and linewidth in FeSe are very sensitive to any static local-field contribution. We determine the Knight shift from the first spectral moment of our data, using a nuclear gyromagnetic ratio $\gamma(^{77}\text{Se})/2\pi = 8.13$ MHz/T. The ^{77}Se NMR spectra yield a typical linewidth (FWHM) of about 3 kHz, in line with previously reported results [8, 9]. We take the FWHM as very conservative error for the Knight-shift data, see Fig. 2.

For precise determination of the ^{77}Se Knight shift, the magnetic field was repeatedly calibrated with a ^{63}Cu NMR reference during the experiments. For all fields, the temperature dependence of the Knight shift shows no noticeable change below 30 K, see Fig. 2(c). It increases only for $T \geq 30$ K, consistent with previous reports [8, 9]. In particular, the ^{77}Se NMR spectra recorded at 0.3 K, deep in the superconducting state, yield, within error bars, no decrease of the shift within the whole field range of our measurements, including the transition between A

and B phase [Fig. 2(d)]. This is quite surprising, since, in a spin-singlet superconductor, a reduction of the local spin susceptibility, driven by the formation of Cooper pairs, occurs when approaching zero field at temperatures much smaller than T_c. Therefore, we conclude that the observed Knight shift of about 1300 ppm is purely of orbital origin, and that the static uniform electronic spin susceptibility in FeSe is extremely small at temperatures approaching the superconducting state.

This finding is further corroborated by the very small linewidth and purely Lorentzian NMR lineshape in the whole parameter range of our study. Any finite contribution from local susceptibilities would, with the large ^{77}Se hyperfine coupling mentioned above, immediately lead to Gaussian line broadening. Also, the linewidth of the Redfield pattern, resulting from a periodic array of local orbital magnetization in the vortex lattice, is estimated to be much smaller than the linewidth of the ^{77}Se spectra in the high-field regime of our study [31]. A recent study of anisotropic spectral properties in the superconducting state of FeSe reports results in agreement with our findings, as well as a rather small suppression of the Knight shift and inhomogeneously broadened spectra below T_c for in-plane fields [32]. With the given hyperfine coupling and linewidth, we estimate the upper limit of the uniform static susceptibility for fields parallel c to about 2×10^{-5} emu/(G mol). Further, our findings confirm that the splitting of the ^{77}Se line, observed for fields applied along the ab planes and interpreted as a microscopic signature of nematic order in FeSe, stems from the anisotropic orbital polarization in the orbital-ordered domains [8, 9]. A study by means of ^{77}Se NMR and microscopic modeling on detwinned FeSe in the nematic state reports that the static magnetic susceptibility at the wave vector $q = 0$ is mainly of orbital character, whereas the spin part dominates at $q = (\pi, 0)$ and $(0, \pi)$, in agreement with our observations [33].

Next, we turn to the discussion of the low-energy spin fluctuations. As shown in Fig. 3(a), for $T > 10$ K, $1/T_1T$ is only weakly field dependent, in good agreement with previous results [6, 8, 9, 34]. For decreasing $T < 10$ K and $\mu_0 H < 13$ T, we find a decrease of $1/T_1T$, clearly starting from well above T_c. These results are in line with recent reports of pre-formed Cooper pairs and associated pseudogap behavior, leading to a depletion of the density of states above the superconducting condensation temperature [6, 34]. The pseudogap sets in below about 10 K, whereas the spin part of the Knight shift decreases already at higher temperatures [see Fig. 2(c)], finally becoming smaller than the spectroscopic linewidth below 30 K. Consequently, the decrease of the static spin susceptibility is not related to the pseudogap formation.

Upon crossing the superconducting transition, $1/T_1T$ drops further - without showing any feature that might be associated with T_c - and levels off at about 2 K at 11 T and 3 K at 8 T, in good agreement with the vortex liquid-solid transition indicated by the peak fields obtained from the torque data reported by Kasahara et al. [21], as well as our RF reflection measurements. At lower temperatures, $1/T_1T$ is almost constant, and increases with magnetic field. For higher magnetic fields, at 13 T, the relaxation rate does not decrease below T_c, and finally, at 15 T, despite the transition to superconductivity as probed by the abrupt decrease of the NMR signal intensity (cf. inset of Fig. 1), $1/T_1T$ even monotonically increases towards lowest temperatures. These observations are in line with a field-driven suppression of the pseudogap, being associated with preformed pairs of the superconducting condensate, as predicted for the BCS-BEC crossover regime [6, 23].

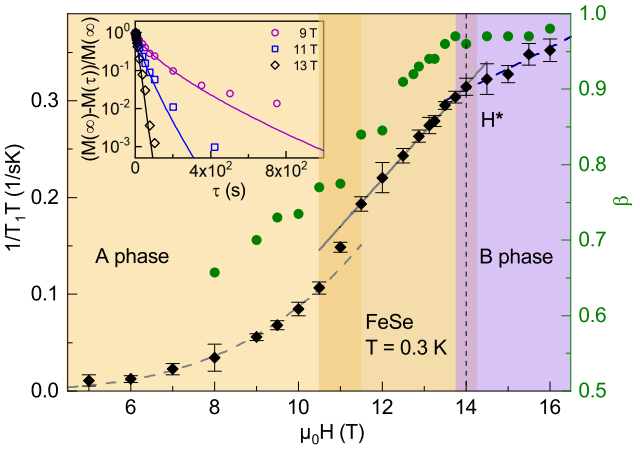

FIG. 4. Magnetic-field dependence of $1/T_1T$ (diamonds) and the corresponding stretching exponent (circles) at 0.3 K, deep in the superconducting state of FeSe. Dashed lines are guides to the eye. The vertical dashed line denotes the transition field H^* between A and B phases. The inset shows selected T_1 relaxation data with the corresponding fits in a semi-logarithmic plot, the stretched behavior clearly decreases with increasing field.

In Fig. 3(b), the temperature dependence of the stretching exponent β is shown for 11 and 15 T. In the normal-conducting state, we find $\beta \approx 1$, indicating a single T_1 and correspondingly a spatially homogeneous electronic state in the whole sample volume. At 11 T, when entering the A phase, β becomes smaller than unity below T_c, in line with the presence of a vortex lattice with superconducting regions and vortex cores with increased quasiparticle density. In stark contrast, at 15 T, in the B phase, β remains close to unity at temperatures below T_c, evidencing a spatially homogeneous electronic state.

The field dependence of $1/T_1T$ at 0.3 K (Fig. 4), deep in the superconducting state, is determined both by the structure of the vortex lattice and the gradual suppression of the superconducting gap amplitudes. Again, the presence of a vortex lattice gives rise to a spatial variation of quasiparticle densities, yielding a distribution of T_1 relaxation times with β becoming smaller than unity [31, 35]. Towards high fields, the superconducting gap amplitudes decrease, and the vortex density with the corresponding volume fraction of the normal-conducting

vortex cores increases. In consequence, the overall T_1 distribution sharpens, and β approaches unity.

The field dependence of $1/T_1T$ yields two transitional regimes at around 11 and 14 T, respectively. As was reported from measurements of the thermal Hall coefficients, the transverse thermal conductivity changes sign at around 12 T and 0.59 K, indicating that the quasiparticles that determine the thermal conduction change from electron-like to hole-like [22]. The clear change in the field dependence of $1/T_1T$ at around 11 T is likely driven by the same phenomenon, namely, a field-driven closure of the smaller, anisotropic gap on the electron pocket. Here, the field-dependent increase of β shows a monotonic variation of the spatial dependence of the low-energy quasiparticle density.

The second change of the field dependence of $1/T_1T$ occurs around $\mu_0H^\star \approx 14$ T, which gives evidence of a field-driven transition to a distinct bulk superconducting state, in very good agreement with features found in previous reports based on thermodynamic quantities [21, 22]. Above 14 T, in the B phase, the field dependence of $1/T_1T$ becomes approximately linear with a significantly smaller slope, without saturation up to 16 T. More importantly, the stretching exponent β saturates close to unity above 14 T, evidencing spatially homogeneous low-energy quasiparticle excitations. Since the magnetic-torque measurements show no anomaly at $\mu_0H^\star$, a Lifshitz transition or spin-density wave order as driving mechanism for the transition to the B phase are very unlikely [21].

Finally, we comment on the compatibility of our results with an FFLO state underlying the B phase [21, 22]. The spectroscopic signature of a spatially inhomogeneous superconducting state, as predicted by FFLO, with coupled modulated local susceptibility, would be an inhomogeneous broadening of the spectral line. This was observed in NMR studies of the FFLO states in the organic superconductors κ-$(ET)_2Cu(NCS)_2$ [36] and β''-$(ET)_2SF_5CH_2CF_2SO_3$ [37]. However, as K_s is smaller than the ^{77}Se linewidth in FeSe, a corresponding modulation would not be resolved. As to the dynamic properties, a spatially inhomogeneous superconducting state would give rise to a local variation of the quasiparticle densities and result in a stretched relaxation, unless strong mechanisms of nuclear spin diffusion are at play. However, spatial inhomogeneities arising from an FFLO state are in contrast to our observations of $\beta = 1$ for the B phase. We, therefore, may exclude a simple FFLO state as origin for the B phase.

IV. SUMMARY

In summary, RF volume penetration and ^{77}Se NMR measurements of the static and low-energy dynamic susceptibility of single-crystalline FeSe at fields between 5 and 16 T and temperatures down to 0.3 K reveal that the high-field B phase represents a distinct bulk superconducting state of a highly spin-polarized Fermi liquid with nonlinear RF response of the surface conductivity. The B phase yields, within our experimental resolution, no spatial modulation of either the density of low-energy quasiparticle excitations or the static local susceptibility, as evidenced by a non-stretched spin-lattice relaxation and the absence of a discernible inhomogeneous line broadening, respectively. Rather, $1/T_1T$ increases monotonically towards low temperatures and increasing fields in the B phase, which sets it apart from standard BCS bulk superconductivity with gapped excitations. Further, measurements of the orbital part of the NMR Knight shift deep in the superconducting state reveal that the static spin susceptibility in FeSe becomes extremely small below 30 K, despite the presence of pronounced spin fluctuations. In line with previous results, $1/T_1T$ reveals a gapped behavior of the low-energy spin fluctuations already well above T_c in a wide field range, indicating pseudo-gap formation due to preformed Cooper pairs, which underlines the unusual superconductivity of FeSe in the BCS-BEC crossover regime.

ACKNOWLEDGMENTS

We thank Y. Matsuda, S.-L. Drechsler, V. Grinenko, S. Arsenijević, and S. Kasahara for valuable discussions. We acknowledge support from the Deutsche Forschungsgemeinschaft (DFG) through GRK 1621 and the Würzburg-Dresden Cluster of Excellence on Complexity and Topology in Quantum Matter–*ct.qmat* (EXC 2147, Project No. 390858490), as well as by the HLD at HZDR, a member of the European Magnetic Field Laboratory (EMFL). Z.T.Z. was financially supported by the National Natural Science Foundation of China (Grant No. 11304321) and by the International Postdoctoral Exchange Fellowship Program 2013 (Grant No. 20130025).

[1] Y. J. Kamihara, T. Watanabe, M. Hirano, and H. Hosono, J. Am. Chem. Soc. **130**, 3296 (2008).
[2] D. Johnston, Adv. Phys. **59**, 803 (2010).
[3] G. R. Stewart, Rev. Mod. Phys. **83**, 1589 (2011).
[4] A. Chubukov and P. Hirschfeld, Physics Today **68**, 46 (2015).
[5] F.-C. Hsu, J.-Y. Luo, K.-W. Yeh, T.-K. Chen, T.-W. Huang, P. M. Wu, Y.-C. Lee, Y.-L. Huang, Y.-Y. Chu, D.-C. Yan, and M.-K. Wu, Proc. Natl. Acad. Sci. USA **105**, 14262 (2008).
[6] S. Kasahara, T. Yamashita, A. Shi, R. Kobayashi, Y. Shimoyama, T. Watashige, K. Ishida, T. Terashima, T. Wolf, F. Hardy, C. Meingast, H. v. Löhneysen, A.

Levchenko, T. Shibauchi, and Y. Matsuda, Nat. Commun. **7**, 12843 (2016).
[7] P. Bourgeois-Hope, S. Chi, D. A. Bonn, R. Liang, W. N. Hardy, T. Wolf, C. Meingast, N. Doiron-Leyraud, and L. Taillefer, Phys. Rev. Lett. **117**, 097003 (2016).
[8] S. H. Baek, D. V. Efremov, J. M. Ok, S. J. Kim, J. v. d. Brink, and B. Büchner, Nat. Mater. **14**, 210 (2015).
[9] A. E. Böhmer, T. Arai, F. Hardy, T. Hattori, T. Iye, T. Wolf, H. v. Löhneysen, K. Ishida, and C. Meingast, Phys. Rev. Lett. **114**, 027001 (2015).
[10] Q. Wang, Y. Shen, B. Pan, Y. Hao, M. Ma, F. Zhou, P. Steffens, K. Schmalzl, T. R. Forrest, M. Abdel-Hafiez, X. Chen, D. A. Chareev, A. N. Vasiliev, P. Bourges, Y. Sidis, H. Cao, and J. Zhao, Nat. Mater. **15** 159 (2016).
[11] F. Wang, S. A. Kivelson, and D.-H. Lee, Nat. Phys. **11**, 959 (2015).
[12] J. M. Ok, C. I. Kwon, Y. Kohama, J. S. You, S. K. Park, J. H. Kim, Y. J. Jo, E. S. Choi, K. Kindo, W. Kang, K. S. Kim, E. G. Moon, A. Gurevich, and J. S. Kim, Phys. Rev. B **101**, 224509 (2020).
[13] V. Grinenko, R. Sarkar, P. Materne, S. Kamusella, A. Yamamshita, Y. Takano, Y. Sun, T. Tamegai, D. V. Efremov, S.-L. Drechsler, J.-C. Orain, T. Goko, R. Scheuermann, H. Luetkens, and H.-H. Klauss, Phys. Rev. B **97**, 201102(R) (2018).
[14] J. Li, B. Lei, D. Zhao, L. P. Nie, D. W. Song, L. X. Zheng, S. J. Li, B. L. Kang, X. G. Luo, T. Wu, and X. H. Chen, Phys. Rev. X **10**, 011034 (2020).
[15] S. Kasahara, Y. Sato, S. Licciardello, M. Čulo, S. Arsenijević, T. Ottenbros, T. Tominaga, J. Böker, I. Eremin, T. Shibauchi, J. Wosnitza, N. E. Hussey, and Y. Matsuda, Phys. Rev. Lett. **124**, 107001 (2020).
[16] T. Terashima, N. Kikugawa, A. Kiswandhi, E.-S. Choi, J. S. Brooks, S. Kasahara, T. Watashige, H. Ikeda, T. Shibauchi, Y. Matsuda, T. Wolf, A. E. Böhmer, F. Hardy, C. Meingast, H. v. Löhneysen, M. T. Suzuki, R. Arita, and S. Uji, Phys. Rev. B. **90**, 144517 (2014).
[17] A. E. Böhmer and C. Meingast, Comptes Rendus Physique **17**, 90 (2016).
[18] S. Medvedev, T. M. McQueen, I. A. Troyan, T. Palasyuk, M. I. Eremets, R. J. Cava, S. Naghavi, F. Casper, V. Ksenofontov, G. Wortmann, and C. Felser, Nat. Mater. **8**, 630 (2009).
[19] S. He, J. He, W. Zhang, L. Zhao, D. Liu, X. Liu, D. Mou, Y.-B. Ou, Q.-Y. Wang, Z. Li, L. Wang, Y. Peng, Y. Liu, C. Chen, L. Yu, G. Liu, X. Dong, J. Zhang, C. Chen, Z. Xu, X. Chen, X. Ma, Q. Xue, and X. J. Zhou, Nat. Mater. **12**, 605 (2013).
[20] J.-F. Ge, Z.-L. Liu, C. Liu, C.-L. Gao, D. Qian, Q.-K. Xue, Y. Liu, and J.-F. Jia, Nat. Mater. **14**, 285 (2015).
[21] S. Kasahara, T. Watashige, T. Hanaguri, Y. Kohsaka, T. Yamashita, Y. Shimoyama, Y. Mizukami, R. Endo, H. Ikeda, K. Aoyama, T. Terashima, S. Uji, T. Wolf, H. v. Löhneysen, T. Shibauchi, and Y. Matsuda, Proc. Natl. Acad. Sci. USA **111**, 16309 (2014).
[22] T. Watashige, S. Arsenijević, T. Yamashita, D. Terazawa, T. Onishi, L. Opherden, S. Kasahara, Y. Tokiwa, Y. Kasahara, T. Shibauchi, H. v. Löhneysen, J. Wosnitza, and Y. Matsuda, J. Phys. Soc. Jpn. **86**, 014707 (2017).
[23] M. Randeria and E. Taylor, Annu. Rev. Condens. Matter Phys. **5**, 209 (2014).
[24] A. E. Böhmer, F. Hardy, F. Eilers, D. Ernst, P. Adelmann, P. Schweiss, T. Wolf, and C. Meingast, Phys. Rev. B **87**, 180505(R) (2013).
[25] See Supplemental material at [URL will be inserted by publisher] for ^{77}Se NMR nutation and thermal-conductivity experiments in the normal and superconducting states, as well as more details on the spectroscopic properties.
[26] M. Li, N. R. Lee-Hone, S. Chi, R. Liang, W. N. Hardy, D. A. Bonn, E. Girt, and D. M. Broun, New J. Phys. **18**, 082001 (2016).
[27] N. Terasaki, H. Mukuda, M. Yashima, Y. Kitaoka, K. Miyazawa, P. M. Shirage, H. Kito, H. Eisaki, and A. Iyo, J. Phys. Soc. Jpn. **78**, 013701 (2009).
[28] K. Kitagawa, N. Katayama, K. Ohgushi, M. Yoshida, and M. Takigawa, J. Phys. Soc. Jpn. **77**, 114709 (2008).
[29] K. Kitagawa, N. Katayama, K. Ohgushi, M. Takigawa, J. Phys. Soc. Jpn. **78**, 063706 (2009).
[30] S.-H. Baek, H.-J. Grafe, F. Hammerath, M. Fuchs, C. Rudisch, L. Harnagea, S. Aswartham, S. Wurmehl, J. v. d. Brink, and B. Büchner, Eur. Phys. J. B **85**, 1 (2012).
[31] N. J. Curro, Rep. Prog. Phys. **72**, 026502 (2009).
[32] I. Vinograd, S. P. Edwards, Z. Wang, T. Kissikov, J. K. Byland, J. R. Badger, V. Taufour, and N. J. Curro, arXiv.org, 2102.09090 (2021).
[33] R. Zhou, D. D. Scherer, H. Mayaffre, P. Toulemonde, M. Ma, Y. Li, B. M. Andersen, and M.-H. Julien, npj Quantum Mater. **5**, 93 (2020).
[34] A. Shi, T. Arai, S. Kitagawa, T. Yamanaka, K. Ishida, A. E. Böhmer, C. Meingast, T. Wolf, M. Hirata, and T. Sasaki, J. Phys. Soc. Jpn. **87**, 013704 (2018).
[35] D. C. Johnston, Phys. Rev. B **74**, 184430 (2006).
[36] J. A. Wright, E. Green, P. Kuhns, A. Reyes, J. Brooks, J. Schlueter, R. Kato, H. Yamamoto, M. Kobayashi, and S. E. Brown, Phys. Rev. Lett. **107**, 087002 (2011).
[37] G. Koutroulakis, H. Kühne, J. A. Schlueter, J. Wosnitza, and S. E. Brown, Phys. Rev. Lett. **116**, 067003 (2016).